GeoScienceWorld
Lithosphere
Volume 2021, Article ID 6669012, 19 pages
https://doi.org/10.2113/2021/6669012

Lithosphere

Research Article

Dynamic Material Balance Method for Estimating Gas in Place of Abnormally High-Pressure Gas Reservoirs

Lixia Zhang,[1] **Yingxu He**,[2] **Chunqiu Guo**,[1] **and Yang Yu**[1]

[1]*Research Institute of Petroleum Exploration and Development, PetroChina, Beijing 100083, China*
[2]*Bohai Oilfield Research Institute, Tianjin Branch of CNOOC (China) Limited, Tianjin 300459, China*

Correspondence should be addressed to Lixia Zhang; zhanglixia2016@petrochina.com.cn

Received 11 December 2020; Accepted 4 February 2021; Published 10 March 2021

Academic Editor: Zhongwei Wu

Determination of gas in place (GIP) is among the hotspot issues in the field of oil/gas reservoir engineering. The conventional material balance method and other relevant approaches have found widespread application in estimating GIP of a gas reservoir or well-controlled gas reserves, but they are normally not cost-effective. To calculate GIP of abnormally pressured gas reservoirs economically and accurately, this paper deduces an iteration method for GIP estimation from production data, taking into consideration the pore shrinkage of reservoir rock and the volume expansion of irreducible water, and presents a strategy for selecting an initial iteration value of GIP. The approach, termed DMBM-APGR (dynamic material balance method for abnormally pressured gas reservoirs) here, is based on two equations: dynamic material balance equation and static material balance equation for overpressured gas reservoirs. The former delineates the relationship between the quasipressure at bottomhole pressure and the one at average reservoir pressure, and the latter reflects the relationship between average reservoir pressure and cumulative gas production, both of which are rigidly demonstrated in the paper using the basic theory of gas flow through porous media and material balance principle. The method proves effective with several numerical cases under various production schedules and a field case under a variable rate/variable pressure schedule, and the calculation error of GIP does not go beyond 5% provided that the production data are credible. DMBM-APGR goes for gas reservoirs with abnormally high pressure as well as those with normal pressure in virtue of its strict theoretical foundation, which not only considers the compressibilities of rock and bound water, but also reckons with the changes in production rate and variations of gas properties as functions of pressure. The method may serve as a valuable and reliable tool in determining gas reserves.

1. Introduction

The determination of gas in place, as a basic problem in the field of oil and gas reservoir engineering, is related to the development planning and production design of gas wells. Common methods to estimate reserves include volumetric method [1], material balance method [2], transient well test analysis [3, 4], and production decline analysis [5–7], where the first two approaches are usually applied to gas field or gas reservoir, while pressure transient analysis and rate transient analysis are mainly used to calculate well controlled reserves.

A variety of existing GIP determination methods based on the material balance equation, unfortunately, are inconvenient and uneconomical to implement owing to the demand for accurate average formation pressure data often obtained by shutting-in the wells or well testing. Therefore, many researchers turn to the investigation of production data-driven methods for calculating GIP or gas reserves.

For gas reservoirs without water drive, Mattar and McNeil (1995, 1998) [8, 9] proposed the flowing material balance procedure when the gas well is flowing at a constant rate. It is, however, less desirable to obtain convincing results because the variations of gas property parameters (such as gas viscosity and compressibility factor or Z-factor) with pressure or time are not considered.

Blasingame and Lee (1988) [10] presented the variable rate reservoir limits testing of gas wells, a new method of estimating GIP from production data (bottomhole pressures, flow rates, and cumulative gas production), based on the

theory of gas flow derived from slightly compressible liquid solution and the introduction of material balance quasitime function t_{ca}. The method combines the gas flow equation (that is an approximation for variable rate and post-transient flow) with the material balance equation (MBE) of volumetric gas reservoirs, and requires a computer program to iterate on average reservoir pressure and material balance quasitime. Nevertheless, it does not consider the effects from characteristics of geopressured gas reservoirs nor explain how to select the initial value.

Mattar and Anderson (2005, 2006) [11, 12] developed the concept of variable rate flowing material balance or "dynamic material balance" extending the flowing material balance method to cases where the production rate is not constant and correspondingly flowing pressure is also variable. Like the treating process of Blasingame and Lee [10], the dynamic material balance procedure, derived from MBE of volumetric gas reservoirs and gas flow equation for boundary-dominated flow (or stabilized flow), also needs a calculation program to iterate on gas in place. On account of the use of pseudovariables (i.e., pseudopressure and pseudotime) accounting for the pressure-dependent changes in gas properties, Matter's dynamic material balance procedure seemingly has a more rigorous theoretical basis than the previous flowing material balance, but it does not incorporate compressibilities of rock and irreducible water yet.

Material balance analysis of production performance for an overpressured gas reservoir is complicated because of the influence of rock and water compressibility in addition to significant gas compressibility effects. This makes it vital to include both formation and water compressibility in the production performance analysis when trying to estimate GIP of abnormally pressured reservoirs. In general, the traditional material balance equation or related methods can be directly used to calculate GIP, whereas well shutdown or well testing to determine the average reservoir pressure results in loss of production and expensive cost. Alternatively, those methods using production data [13–17] almost do not reckon in the characteristic of abnormally pressured gas reservoirs, a fact that the elastic effects of rock pore and irreducible water are often not negligible as the formation pressure decreases [18, 19]. Therefore, this paper, taking the pore reduction in reservoir rock and the volume increase in bound water into account, develops an iterative calculation technique for determining gas in place of abnormally pressured gas reservoirs, an improvement of Matter's dynamic material balance, based on a new total compressibility definition and the new material balance equation. The dynamic material balance equation (DMBE) is rigorously derived from the gas flow theory with variable rates; then, it is applied to GIP determination coupled with the material balance principle of overpressured gas reservoirs.

The layout of this article is as follows. First, the gas flow model for a closed gas reservoir with abnormally high pressure is introduced and solved in order to obtain the dynamic material balance equation. Second, the corresponding static material balance equation is presented which is then coupled with DMBE to compute average reservoir pressure. Third, the iterative method (DMBM-APGR) for GIP estimation is developed and the detailed iteration steps are described. Fourth, several case studies illustrate and validate the method, and a brief discussion reveals the novelties of the work. Finally, conclusions are drawn.

2. Mathematical Model of Gas Flow through Porous Media

When it comes to the problem of liquid flow through porous media, the comprehensive differential equation (governing equation) is a typical diffusivity equation where the diffusivity coefficient can be approximately seen as a constant; thus, it is easy to solve; but for gas flow, the situation is quite different in that the linearization of the corresponding diffusivity equation is essential to consider the pressure-dependent changes in gas properties such as viscosity, Z-factor, and compressibility.

The key to solve the gas flow problem is the linearization of the diffusivity equation. Al-Hussainy et al. (1966) [20, 21] and Russell et al. (1966) [22] took the lead in scoring representative research results in this field. The concept of "pseudopressure" proposed by them can partially linearize the gas flow diffusivity equation. The pseudopressure presented by Russell et al. (1966) is, in fact, a normalized pseudopressure with the dimension of pressure.

Agarwal (1979) [23] proposed the concept of pseudotime, representing a new stage for solution of gas flow. Lee and Holditch (1982) [24] pointed out that the application of pseudopressure and pseudotime can effectively linearize the gas diffusivity equation, and it is feasible to apply the slightly compressible liquid solution to gas flow.

Fraim and Wattenbarger (1987) [25], introducing the real gas pseudopressure and a normalized time function, investigated the gas flow problem for a closed gas reservoir producing against constant wellbore pressure during boundary-dominated flow, where the normalized time should adopt the viscosity and compressibility at the average reservoir pressure rather than the bottomhole pressure.

The concepts of quasipressure and quasitime put forward by Meunier et al. (1984, 1987) [26, 27] retain the dimensions of real pressure and real time, and are also known as normalized pseudopressure and normalized pseudotime, respectively, more convenient to use than before.

In addition, some researchers [28, 29] employ the time-dependent dimensionless viscosity-compressibility ratio λ, the time-averaged λ (i.e., $\bar{\lambda}$), and gas density to approximately and successfully linearize the density-diffusivity equation for unsteady state analysis of natural gas reservoirs. This density-based approach, in fact, can be expressed as the counterpart mathematically equivalent to the pseudofunction-based approach for the gas flow diffusivity equation.

In this section, firstly, the gas flow model including water, rock, and gas compressibility effects is established on the basis of the mass conservation principle and state equations. Secondly, the constant rate solution for the gas flow model is obtained using Laplace transform and liquid-based analytical solutions rewritten in terms of quasivariables. Then, the variable rate solution is also acquired according to the principle of quasipressure drop superposition. Finally, the dynamic

material balance equation for abnormally pressured gas reservoirs is proved based on the definition of average reservoir quasipressure and the preceding variable rate solution.

2.1. Gas Flow Governing Equation. The principle of continuity for gas flow through porous media in its differential form can be expressed as follows:

$$-\left[\frac{\partial\left(\rho_g v_x\right)}{\partial x}+\frac{\partial\left(\rho_g v_y\right)}{\partial y}+\frac{\partial\left(\rho_g v_z\right)}{\partial z}\right]+q_g=\frac{\partial\left[\rho_g(1-S_{wc})\phi\right]}{\partial t}, \tag{1}$$

where ρ_g (kg/m^3) denotes the gas density, v_x, v_y, v_z represent the component of velocity in the x, y, z directions, respectively, ϕ is the porosity, q_g [kg/(m^3·s)] denotes the change in fluid mass caused by the source or sink in the unit volume per unit time, S_{wc} denotes the irreducible water saturation, and t (s) is the time.

The continuity equation of single-phase gas flow without source/sink term is as follows:

$$-\nabla\cdot\left(\rho_g\vec{v}_g\right)=(1-S_{wc})\frac{\partial\left(\rho_g\phi\right)}{\partial t}+\rho_g\phi\frac{\partial(1-S_{wc})}{\partial t}. \tag{2}$$

Without regard to the non-Darcy effect by high flow velocity, or the additional threshold pressure gradient by the presence of adsorption or hydration films on the rock surface, the gas flow is subject to Darcy's law:

$$\vec{v}_g=-\frac{K}{\mu}\nabla p, \tag{3}$$

where $\vec{v}_g$ (m/s) is the gas velocity vector, μ (Pa·s) denotes the gas viscosity, K (m^2) denotes the effective permeability, and p (Pa) represents the pressure.

According to the definition of rock compressibility, we obtain the following:

$$C_\phi=\frac{1}{V_p}\cdot\frac{dV_p}{dp}=\frac{1}{\phi}\cdot\frac{d\phi}{dp}, \tag{4}$$

where C_ϕ (Pa^{-1}) denotes the rock compressibility and V_p (m^3) represents the pore volume.

Integrating above Equation (4) with respect to p yields porosity and pore volume given by the following:

$$\begin{aligned}\phi&=\phi_i\cdot e^{C_\phi(p-p_i)},\\ V_p&=V_{pi}\cdot e^{C_\phi(p-p_i)},\end{aligned} \tag{5}$$

where p_i (Pa) denotes the initial reservoir pressure; ϕ_i and V_{pi} (m^3) represents the porosity and pore volume under initial reservoir condition, respectively.

Isothermal compressibility of natural gas and gas density can be written as follows:

$$C_g=\frac{ZT}{p}\cdot\frac{d}{dp}\left(\frac{p}{ZT}\right)=\frac{Z}{p}\cdot\frac{d}{dp}\left(\frac{p}{Z}\right), \tag{6}$$

$$\rho_g=\frac{pM}{ZRT}, \tag{7}$$

where C_g (Pa^{-1}) denotes the gas isothermal compressibility, Z represents the deviation factor (Z-factor), T (K) is the temperature, M (kg/mol) denotes the gas molar mass, and R [8.3144598 J/(mol·k)] denotes the molar gas constant [30, 31].

According to the definition of water compressibility, there is

$$C_w=-\frac{1}{V_w}\cdot\frac{dV_w}{dp}. \tag{8}$$

By separating variables and integrating Equation (8) with respect to p, one obtains the following:

$$V_w=V_{wi}\cdot e^{-C_w(p-p_i)}. \tag{9}$$

Then, the bound water saturation is given by the following:

$$S_{wc}=\frac{V_w}{V_p}=\frac{V_{wi}\cdot e^{-C_w(p-p_i)}}{V_{pi}\cdot e^{C_\phi(p-p_i)}}=S_{wci}\cdot e^{-\left(C_w+C_\phi\right)(p-p_i)}, \tag{10}$$

where V_w (m^3) denotes the volume of bound water, V_{wi} represents the initial volume of bound water, C_w (Pa^{-1}) is the water compressibility, and S_{wci} is the initial bound water saturation.

Substituting Equations (3), (5), (6), (7), and (10) into Equation (2), the rearranged equation is represented by the following:

$$\nabla\cdot\left(\frac{p}{\mu Z}\nabla p\right)=\frac{\phi_i\mu C_t}{K}\cdot\frac{p}{\mu Z}\frac{\partial p}{\partial t}, \tag{11}$$

$$C_t=e^{C_\phi(p-p_i)}\left[C_\phi+(1-S_{wc})C_g+S_{wc}C_w\right]. \tag{12}$$

Equation (11) is the governing equation of unsteady single-phase gas flow in which gas property parameters (μ, Z, and C_t) are not constant and change with pressure. Thus, it is difficult to solve it directly. Referring to the concepts of pseudopressure proposed by Russell et al. (1966) [22] and quasitime developed by Meunier et al. (1984, 1987) [26, 27], quasivariables in this paper are defined by the following:

$$p_p=p_i+\frac{\mu_i}{\rho_{gi}}\int_{p_i}^{p}\frac{\rho_g(\xi)}{\mu(\xi)}d\xi=p_i+\frac{\mu_i Z_i}{p_i}\int_{p_i}^{p}\frac{\xi}{\mu(\xi)Z(\xi)}d\xi, \tag{13}$$

$$t_a=\mu_i C_{ti}\int_0^t\frac{1}{\mu C_t}dt, \tag{14}$$

where p_p (Pa) denotes the quasipressure function, t_a (s)

denotes the quasitime function, and C_t (Pa^{-1}) denotes the total compressibility function defined by Equation (12); μ_i, Z_i, ρ_{gi}, and C_{ti} represent the gas viscosity, deviation factor, density, and total compressibility under initial reservoir condition, respectively.

Based on Equations (13) and (14), then Equation (11) can be transformed into the following:

$$\nabla^2 p_p = \frac{\phi_i \mu_i C_{ti}}{K} \cdot \frac{\partial p_p}{\partial t_a}. \tag{15}$$

Equation (15) is characterized by the similar form of the diffusivity equation for liquid flow. It could be seen that the form of expression for gas flow behaviors is consistent with that of liquid based on the definitions of quasivariables in the paper, so the slightly compressible liquid solution could be applied to gas flow governing equation.

2.2. Constant Rate Solution. The mathematical model of gas flow for a single well producing in a bounded reservoir with a constant production rate can be written as follows:

$$\begin{cases} \dfrac{\partial^2 p_p}{\partial r^2} + \dfrac{1}{r} \cdot \dfrac{\partial p_p}{\partial r} = \dfrac{\phi_i \mu_i C_{ti}}{\alpha_t K} \cdot \dfrac{\partial p_p}{\partial t_a}, \\ \left(r \dfrac{\partial p_p}{\partial r} \right)\Big|_{r=r_w} = \dfrac{q \mu_i B_{gi}}{\alpha_p K h}, \\ \dfrac{\partial p_p}{\partial r}\Big|_{r=r_e} = 0, \\ p_p\Big|_{t_a=0} = p_p(p_i), \end{cases} \tag{16}$$

where r (m) is the distance from a location to the center of the gas well, r_w (m) is the wellbore radius, r_e (m) denotes the reservoir limit, B_{gi} (m^3/m^3) represents the gas formation volume factor under original formation condition, and h (m) denotes the net pay thickness; α_p denotes the conversion factor of dimensionless pressure, and α_t is the conversion factor of dimensionless time. Under the international system of units, $\alpha_p = 2\pi$ and $\alpha_t = 1$; if other unit systems are used, their values are different. For the sake of simplicity, all the symbols in this article are explained in international standard units.

Dimensionless variables for quasipressure, time, and radius are defined by the following:

$$p_D = \frac{\alpha_p K h \left(p_{p_i} - p_p \right)}{q \mu_i B_{gi}}, \tag{17}$$

$$t_D = \frac{\alpha_t \cdot K}{\phi_i \mu_i C_{ti} {r_w}^2} t_a, \tag{18}$$

$$\begin{aligned} r_D &= \frac{r}{r_w}, \\ r_{eD} &= \frac{r_e}{r_w}, \end{aligned} \tag{19}$$

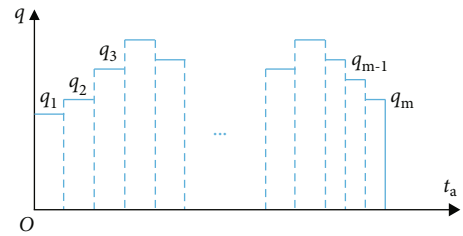

Figure 1: Schematic diagram of variable production rates of a gas well.

where p_D, t_D, and r_D are the dimensionless quasipressure, dimensionless quasitime, and dimensionless radius, respectively; r_{eD} denotes the dimensionless radial length at the reservoir limit.

Substituting Equations (17)–(19) into Equation (16) yields the dimensionless mathematical model of gas flow given by the following:

$$\begin{cases} \dfrac{\partial^2 p_D}{\partial {r_D}^2} + \dfrac{1}{r_D} \dfrac{\partial p_D}{\partial r_D} = \dfrac{\partial p_D}{\partial t_D}, \\ \left(r_D \dfrac{\partial p_D}{\partial r_D} \right)\Big|_{r_D=1} = -1, \\ \dfrac{\partial p_D}{\partial r_D}\Big|_{r_D=r_{eD}} = 0, \\ p_D|_{t_D=0} = 0. \end{cases} \tag{20}$$

From the definitions of quasivariables, it can be easily noted that quasitime t_a is a function of time t, while the gas viscosity μ and total compressibility C_t are the functions of pressure p dependent on location and time; so t_a is a function of location r and time t. Similarly, quasipressure p_p is only related to pressure; therefore, it is also a function of r and t. Strictly speaking, p_p and t_a correspond to the same pressure p, that is, the quasipressure and the quasitime correspond to the same position and the same time, for which we have a fat chance to solve Equations (16) and (20).

The general approach to address the above difficulties, nowadays, is to calculate the value of t_a under a certain reference pressure irrespective of location r, i.e.,

$$t_a = \mu_i C_{ti} \int_0^t \frac{1}{\mu C_t} dt \approx \mu_i C_{ti} \int_0^t \frac{1}{\mu(p_{ref}) C_t(p_{ref})} dt, \tag{21}$$

where p_{ref} represents a reference pressure independent of location.

In this way, t_a is approximately reckoned to be a function merely dependent on time t, so t_D is only related to time, too. The Laplace transform on t_D in Equation (20) enables us to

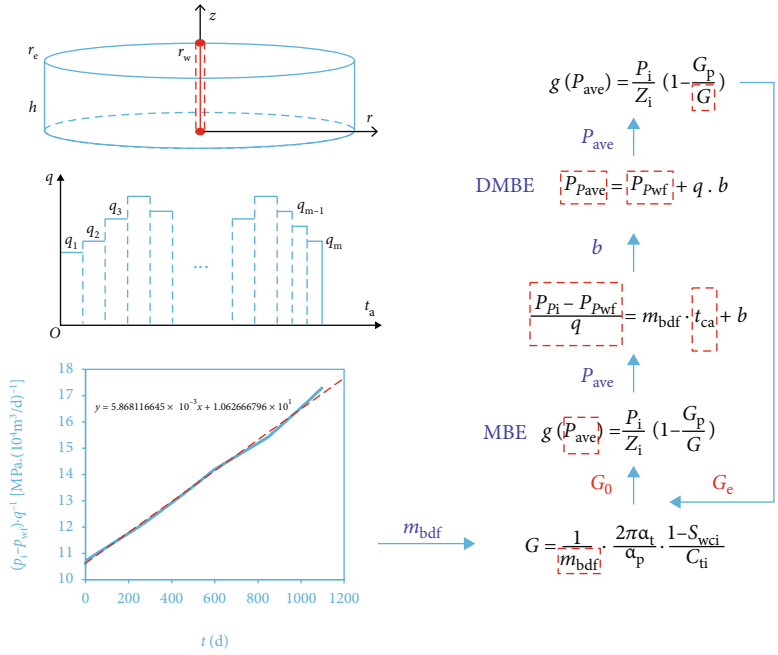

FIGURE 2: The iteration steps of dynamic material balance method for abnormally pressured gas reservoirs.

gain the dimensionless pressure drop p_D which can be expressed as a solution in Laplace domain:

$$\tilde{p}_D = \frac{K_1(r_{eD}\sqrt{s})I_0(r_D\sqrt{s}) + I_1(r_{eD}\sqrt{s})K_0(r_D\sqrt{s})}{s\sqrt{s}\cdot\left[K_1(\sqrt{s})I_1(r_{eD}\sqrt{s}) - K_1(r_{eD}\sqrt{s})I_1(\sqrt{s})\right]}, \quad (22)$$

where $\tilde{p}_D$ denotes the variable in Laplace domain that corresponds to p_D and s is the variable in Laplace domain that corresponds to t_D; I_0 and I_1 are the zero-order and first-order modified Bessel functions of the first kind, respectively; K_0 and K_1 are the zero-order and first-order modified Bessel functions of the second kind, respectively.

The analytical inversion expression of Equation (22) in the real time domain is as follows:

$$\begin{aligned} p_D = {} & \frac{2t_D}{r_{eD}^2 - 1} - \frac{r_{eD}^2}{r_{eD}^2 - 1}\ln r_D \\ & + \frac{4r_{eD}^4 \ln r_{eD} - 3r_{eD}^4 + 2r_D^2(r_{eD}^2 - 1) + 2r_{eD}^2 + 1}{4(r_{eD}^2 - 1)^2} \\ & - \pi\sum_{n=1}^{\infty}\frac{e^{-\lambda_n^2\cdot t_D}\cdot J_1^2(r_{eD}\lambda_n)[Y_1(\lambda_n)J_0(r_D\lambda_n) - J_1(\lambda_n)Y_0(r_D\lambda_n)]}{\lambda_n\cdot\left[J_1^2(r_{eD}\lambda_n) - J_1^2(\lambda_n)\right]}, \end{aligned} \quad (23)$$

where J_0 and J_1 are the zero-order and first-order Bessel functions of the first kind, respectively; Y_0 and Y_1 are the zero-order and first-order Bessel functions of the second kind (Neumann functions), respectively. The variable $\lambda = \lambda_n$ must satisfy the following condition:

$$J_1(r_{eD}\lambda)Y_1(\lambda) - Y_1(r_{eD}\lambda)J_1(\lambda) = 0. \quad (24)$$

2.3. Variable Rate Solution. As shown in Figure 1, there are m times of production fluctuations in the production process of the gas well. According to the principle of pressure drop superposition, the quasipressure drop caused by the changes in production rate can be written as follows:

$$\begin{cases} p_{p_i} - p_p(r, t_a) = \sum_{i=1}^{m}\left(\Delta p_p\right)_i = \sum_{i=1}^{m}\frac{\mu_i B_{gi}}{\alpha_p Kh}\cdot(q_i - q_{i-1})\cdot p_D(t_a - t_{a,i-1}), \\ q_0 = 0, \\ t_{a,0} = 0, \end{cases} \quad (25)$$

where $(\Delta p_p)_i$ represents the quasipressure drop caused by ith production fluctuation, q_i is the production rate during ith production period, q_{i-1} denotes the production rate during (i-1)th production period, and $t_{a,i-1}$ is the quasitime for the start of ith production period.

Combining the definition of dimensionless time Equation (18) with Equations (23) and (25) gives the following:

$$\begin{aligned} p_{p_i} - p_p = {} & \frac{\mu_i B_{gi}}{\alpha_p Kh}\left\{\frac{2}{r_e^2 - r_w^2}\cdot\frac{\alpha_t K}{\phi_i\mu_i C_{ti}}G_{pa}\right. \\ & + \left[-\frac{r_e^2}{r_e^2 - r_w^2}\ln\frac{r}{r_w}\right. \\ & \left.\left. + \frac{4r_e^4\ln(r_e/r_w) - 3r_e^4 + 2r^2(r_e^2 - r_w^2) + 2r_e^2 r_w^2 + r_w^4}{4(r_e^2 - r_w^2)^2}\right]q_m \right. \\ & - \sum_{i=1}^{m}(q_i - q_{i-1})\left[\sum_{n=1}^{\infty}\frac{\pi}{\lambda_n}e^{-\lambda_n^2\cdot(\alpha_t K/\phi_i\mu_i C_{ti}r_w^2)(t_a - t_{a,i-1})}J_1^2\right. \\ & \left.\left.\cdot\left(\frac{r_e}{r_w}\lambda_n\right)\frac{Y_1(\lambda_n)J_0((r/r_w)\lambda_n) - J_1(\lambda_n)Y_0((r/r_w)\lambda_n)}{J_1^2((r_e/r_w)\lambda_n) - J_1^2(\lambda_n)}\right]\right\}, \end{aligned} \quad (26)$$

Table 1: Simulated reservoir and gas properties.

Parameters	Property values	Parameters	Property values
dr	1.5 m	ϕ	0.2
$d\theta$	5°	S_{wci}	0.2
dz	10 m	M_g	19.576754 g/mol
K_r	3 mD	Z_{sc}	0.997514
K_θ	3 mD	C_ϕ	2.364×10^{-3} MPa^{-1}
K_z	0.03 mD	C_w	4.230×10^{-4} MPa^{-1}
p_i	55 MPa	μ_w	0.264565 cp
T_i	381.15 K	μ_i	$3.401434212 \times 10^{-2}$ cp
T_{pc}	201.325729 K	C_{gi}	$8.924326991 \times 10^{-3}$ MPa^{-1}
p_{pc}	4.597109 MPa	C_{ti}	$9.588061593 \times 10^{-3}$ MPa^{-1}
r_e	300 m	B_{gi}	$2.980066777 \times 10^{-3}$ m^3/m^3
r_w	0.1 m	V_{pi}	565864 m^3
h	10 m	G	1.51906310×10^8 m^3

$$G_{pa} = \sum_{i=1}^{m}(q_i - q_{i-1})(t_a - t_{a,i-1}) = \sum_{i=1}^{m} q_i(t_{a,i} - t_{a,i-1}) = \int_0^{t_a} q dt_a. \tag{27}$$

By dividing both ends of Equation (26) by q_m and setting $r_D = 1$, i.e., $r = r_w$, the downhole quasipressure drop correlation is obtained:

$$\begin{aligned}\frac{p_{p_i} - p_{p_{wf}}}{q_m} = \frac{\mu_i B_{gi}}{\alpha_p Kh}\Bigg\{&\frac{2}{r_e^2 - r_w^2}\cdot\frac{\alpha_t K}{\phi_i\mu_i C_{ti}}t_{ca} \\ &+ \frac{4r_e^4\ln(r_e/r_w) - 3r_e^4 + 4r_e^2 r_w^2 - r_w^4}{4(r_e^2 - r_w^2)^2} \\ &- \sum_{i=1}^{m}\frac{q_i - q_{i-1}}{q_m}\left[\sum_{n=1}^{\infty}\frac{\pi}{\lambda_n}e^{-\lambda_n^2\cdot\left(\alpha_t K/\phi_i\mu_i C_{ti} r_w^2\right)(t_a - t_{a,i-1})}J_1^2\right. \\ &\left.\cdot\left(\frac{r_e}{r_w}\lambda_n\right)\frac{Y_1(\lambda_n)J_0(\lambda_n) - J_1(\lambda_n)Y_0(\lambda_n)}{J_1^2((r_e/r_w)\lambda_n) - J_1^2(\lambda_n)}\right]\Bigg\},\end{aligned} \tag{28}$$

$$t_{ca} = \frac{G_{pa}}{q_m} = \frac{1}{q_m}\int_0^{t_a} q dt_a = \frac{1}{q_m}\int_0^{t} q\cdot\frac{\mu_i C_{ti}}{\mu(p_{ref})C_t(p_{ref})}dt, \tag{29}$$

where t_{ca} denotes the material-balance quasitime, G_{pa} represents a variable similar to cumulative gas production defined by Equation (27), $p_{p_{wf}}$ is the quasipressure corresponding to the bottomhole pressure p_{wf}, and p_{p_i} is the quasipressure corresponding to initial reservoir pressure (that is equal to p_i).

For the convenience of writing, the following expression is introduced here:

$$f(t_a, \lambda_n) = \frac{e^{-\lambda_n^2\cdot\left(\alpha_t K/\phi_i\mu_i C_{ti} r_w^2\right)(t_a - t_{a,i-1})}J_1^2((r_e/r_w)\lambda_n)}{J_1^2((r_e/r_w)\lambda_n) - J_1^2(\lambda_n)}. \tag{30}$$

Due to the identical relation [32] given by

$$Y_0(x)J_1(x) - Y_1(x)J_0(x) = \frac{2}{\pi}\cdot\frac{1}{x}, \tag{31}$$

Equation (28) can be transformed into the following:

$$\begin{aligned}\frac{p_{p_i} - p_{p_{wf}}}{q_m} = &\frac{\mu_i B_{gi}}{\alpha_p Kh}\cdot\frac{2}{r_e^2 - r_w^2}\cdot\frac{\alpha_t K}{\phi_i\mu_i C_{ti}}t_{ca} + \frac{\mu_i B_{gi}}{\alpha_p Kh} \\ &\cdot\frac{4r_e^4\ln(r_e/r_w) - 3r_e^4 + 4r_e^2 r_w^2 - r_w^4}{4(r_e^2 - r_w^2)^2} \\ &- \frac{\mu_i B_{gi}}{\alpha_p Kh}\sum_{i=1}^{m}\frac{q_i - q_{i-1}}{q_m}\left[\sum_{n=1}^{\infty}\frac{\pi}{\lambda_n}f(t_a, \lambda_n)\left(-\frac{2}{\pi}\cdot\frac{1}{\lambda_n}\right)\right].\end{aligned} \tag{32}$$

Then, Equation (32) can be rewritten as follows:

$$\begin{aligned}\frac{p_{p_i} - p_{p_{wf}}}{q_m} = &\frac{2\pi\alpha_t}{\alpha_p}\frac{B_{gi}}{\pi(r_e^2 - r_w^2)h\phi_i\cdot C_{ti}}t_{ca} + \frac{\mu_i B_{gi}}{\alpha_p Kh} \\ &\cdot\frac{4r_e^4\ln(r_e/r_w) - 3r_e^4 + 4r_e^2 r_w^2 - r_w^4}{4(r_e^2 - r_w^2)^2} \\ &+ \frac{\mu_i B_{gi}}{\alpha_p Kh}\sum_{i=1}^{m}\frac{q_i - q_{i-1}}{q_m}\left[\sum_{n=1}^{\infty}\frac{2}{\lambda_n^2}\cdot f(t_a, \lambda_n)\right].\end{aligned} \tag{33}$$

The symbols m_{bdf} and b are used to denote the slope and intercept of the straight line in $(\Delta p_p)_{i-wf}/q$ vs. t_{ca} curve, respectively, i.e.,

$$\frac{p_{p_i} - p_{p_{wf}}}{q} = \frac{\left(\Delta p_p\right)_{i\text{-}wf}}{q} = m_{bdf}\cdot t_{ca} + b, \tag{34}$$

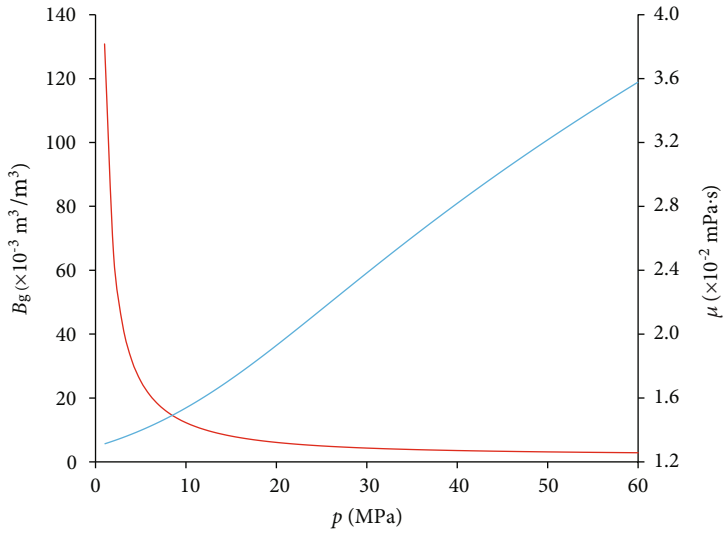

Figure 3: Gas formation volume factor (B_g) and gas viscosity (μ) vs. pressure (p) for numerical cases.

$$m_{\mathrm{bdf}} = \frac{2\pi\alpha_{\mathrm{t}}}{\alpha_{\mathrm{p}}} \cdot \frac{B_{\mathrm{gi}}}{Ah\phi_{\mathrm{i}}C_{\mathrm{ti}}}, \tag{35}$$

$$b = \frac{\mu_{\mathrm{i}}B_{\mathrm{gi}}}{\alpha_{\mathrm{p}}Kh}\left\{\frac{4r_{\mathrm{e}}^{4}\ln\left(r_{\mathrm{e}}/r_{\mathrm{w}}\right) - 3r_{\mathrm{e}}^{4} + 4r_{\mathrm{e}}^{2}r_{\mathrm{w}}^{2} - r_{\mathrm{w}}^{4}}{4\left(r_{\mathrm{e}}^{2} - r_{\mathrm{w}}^{2}\right)^{2}} + \sum_{i=1}^{m}\frac{q_i - q_{i-1}}{q_m}\left[\sum_{n=1}^{\infty}\frac{2}{\lambda_n^{2}}\cdot f\left(t_{\mathrm{a}},\lambda_n\right)\right]\right\}, \tag{36}$$

$$A = \pi\left(r_{\mathrm{e}}^{2} - r_{\mathrm{w}}^{2}\right), \tag{37}$$

where $(\Delta p_p)_{\mathrm{i-wf}}$ represents the difference between the quasi-pressure corresponding to original reservoir pressure p_{i} and that corresponding to bottomhole pressure p_{wf}, and A is the gas reservoir area.

Since transient and stabilized flow [33] may alternate for each production rate change, it can be suggested that stabilized flow will dominate for a small rate change. According to Equation (35), the relationship between gas in place (or well controlled reserves) G and the slope m_{bdf} can be expressed as follows:

$$G = \frac{Ah\phi_{\mathrm{i}}(1 - S_{\mathrm{wci}})}{B_{\mathrm{gi}}} = \frac{1}{m_{\mathrm{bdf}}} \cdot \frac{2\pi\alpha_{\mathrm{t}}}{\alpha_{\mathrm{p}}} \cdot \frac{1 - S_{\mathrm{wci}}}{C_{\mathrm{ti}}}. \tag{38}$$

It is worth noting that once the $(\Delta p_p)_{\mathrm{i-wf}}/q$ vs. t_{ca} graph is drawn and the slope m_{bdf} of the straight line segment is determined, one can calculate GIP based on this slope, which is also the basis for selecting the initial iteration value in the paper. Since $(\Delta p_p)_{\mathrm{i-wf}}/q$ vs. t_{ca} curve cannot be obtained in advance, the authors innovatively use the slope of $(p_{\mathrm{i}} - p_{\mathrm{wf}})/q$ vs. t curve to replace the initial value of m_{bdf}, and GIP estimated by this slope is taken as the initial value of iteration G_0.

It should also be kept in mind that the quasitime t_{a}, in practice, implies a reference pressure independent of location; thus, the material-balance quasitime function t_{ca} is also supposed to be determined at the same reference pressure. At first, Agarwal (1979) [23] and Lee and Holditch (1982) [24] took the bottomhole flowing pressure as the reference pressure, but currently, the reasonable procedure is to adopt the average reservoir pressure [10, 25, 28, 34–36] instead, that is,

$$t_{\mathrm{ca}} = \frac{\mu_{\mathrm{i}}C_{\mathrm{ti}}}{q(t)}\int_0^t \frac{q(t)}{\mu(p_{\mathrm{ave}})C_{\mathrm{t}}(p_{\mathrm{ave}})}dt, \tag{39}$$

where p_{ave} denotes the average reservoir pressure.

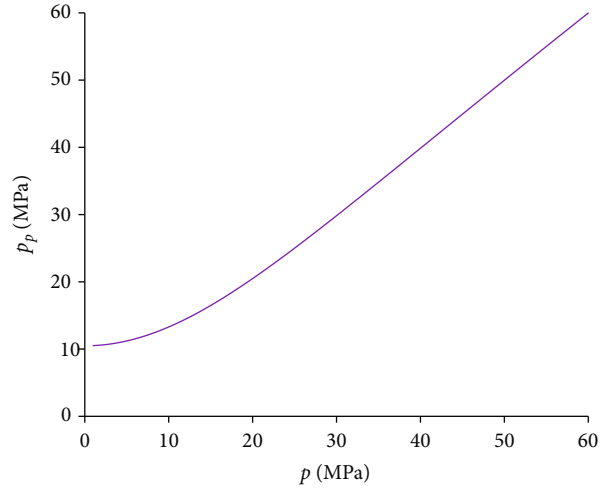

Figure 4: Gas quasipressure function (p_p) vs. pressure (p) for numerical cases.

Table 2: Production schedules for the constant rate case.

t (d)	TS	Δt (h)	Δt (d)	q (10^4 m^3/d)
	1~12	1	0.041667	1.6
	13	3	0.125	1.6
1~1097	14	9	0.375	1.6
	15~16	12	0.5	1.6
	17~1111	24	1	1.6

2.4. Dynamic Material Balance Equation for Abnormally Pressured Gas Reservoirs. By differentiating p_p in Equation (26) with respect to t_a, one obtains the following:

$$-\frac{\partial p_p}{\partial t_a} = \frac{\mu_i B_{gi}}{\alpha_p K h} \cdot \frac{2}{r_e{}^2 - r_w{}^2} \cdot \frac{\alpha_t K}{\phi_i \mu_i C_{ti}} \cdot q_m - \frac{\mu_i B_{gi}}{\alpha_p K h} \times \sum_{i=1}^{m} (q_i - q_{i-1}) \left\{ \sum_{n=1}^{\infty} \frac{\pi}{\lambda_n} f(t_a, \lambda_n) \left[Y_1(\lambda_n) J_0\left(\frac{r}{r_w}\lambda_n\right) - J_1(\lambda_n) Y_0\left(\frac{r}{r_w}\lambda_n\right) \right] \cdot \left(-\lambda_n{}^2 \cdot \frac{\alpha_t K}{\phi_i \mu_i C_{ti} r_w{}^2} \right) \right\}. \tag{40}$$

Then, the governing equation of gas flow can be written as follows:

$$\frac{1}{r}\frac{\partial}{\partial r}\left(r\frac{\partial p_p}{\partial r}\right) = \frac{\phi_i \mu_i C_{ti}}{\alpha_t K}\frac{\partial p_p}{\partial t_a} = -\frac{q_m \mu_i B_{gi}}{\alpha_p K h} \cdot \frac{2}{r_e{}^2 - r_w{}^2} - \frac{\mu_i B_{gi}}{\alpha_p K h} \times \sum_{i=1}^{m} (q_i - q_{i-1}) \cdot \left\{ \sum_{n=1}^{\infty} \frac{\pi \lambda_n}{r_w{}^2} f(t_a, \lambda_n) \left[Y_1(\lambda_n) J_0\left(\frac{r}{r_w}\lambda_n\right) - J_1(\lambda_n) Y_0\left(\frac{r}{r_w}\lambda_n\right) \right] \right\}. \tag{41}$$

Considering

$$\begin{cases} \int r J_0(a \cdot r) dr = \dfrac{r J_1(a \cdot r)}{a}, \\ \int r Y_0(a \cdot r) dr = \dfrac{r Y_1(a \cdot r)}{a}, \end{cases} \tag{42}$$

integrating Equation (41) with respect to r gives the following:

$$r\frac{\partial p_p}{\partial r} = -\frac{q_m \mu_i B_{gi}}{\alpha_p K h}\left(\frac{r^2}{r_e{}^2 - r_w{}^2} + C_1\right) - \frac{\mu_i B_{gi}}{\alpha_p K h} \times \sum_{i=1}^{m} (q_i - q_{i-1}) \left\{ \sum_{n=1}^{\infty} \frac{\pi}{r_w} f(t_a, \lambda_n) \left[Y_1(\lambda_n) r J_1\left(\frac{\lambda_n}{r_w} r\right) - J_1(\lambda_n) r Y_1\left(\frac{\lambda_n}{r_w} r\right) \right] \right\}. \tag{43}$$

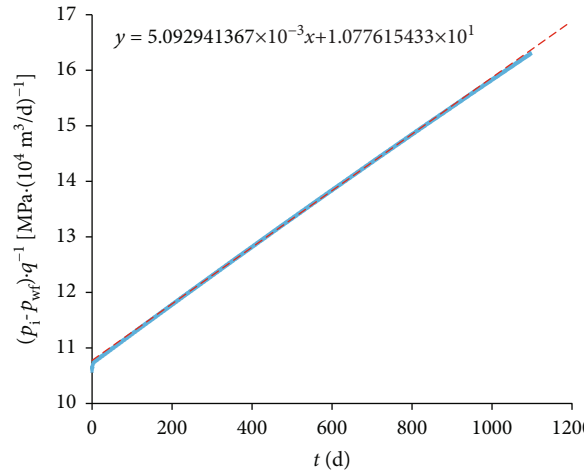

FIGURE 5: $(p_i - p_{wf}) \cdot q^{-1}$ vs. t from real pressure (p) and real time (t) data for the constant flow rate case.

Equation (43) could be rewritten as follows:

$$\frac{\partial p_p}{\partial r} = -\frac{q_m \mu_i B_{gi}}{\alpha_p K h}\left(\frac{r}{r_e{}^2 - r_w{}^2} + \frac{C_1}{r}\right) - \frac{\mu_i B_{gi}}{\alpha_p K h} \times \sum_{i=1}^{m} (q_i - q_{i-1}) \cdot \left\{ \sum_{n=1}^{\infty} \frac{\pi}{r_w} f(t_a, \lambda_n) \left[Y_1(\lambda_n) J_1\left(\frac{\lambda_n}{r_w} r\right) - J_1(\lambda_n) Y_1\left(\frac{\lambda_n}{r_w} r\right) \right] \right\}. \tag{44}$$

The external boundary condition coincides with the following formula:

$$\left.\frac{\partial p_p}{\partial r}\right|_{r=r_e} = -\frac{q_m \mu_i B_{gi}}{\alpha_p K h}\left(\frac{r_e}{r_e{}^2 - r_w{}^2} + \frac{C_1}{r_e}\right) - \frac{\mu_i B_{gi}}{\alpha_p K h} \times \sum_{i=1}^{m} (q_i - q_{i-1}) \cdot \left\{ \sum_{n=1}^{\infty} \frac{\pi}{r_w} f(t_a, \lambda_n) \left[Y_1(\lambda_n) J_1\left(\frac{\lambda_n}{r_w} r_e\right) - J_1(\lambda_n) Y_1\left(\frac{\lambda_n}{r_w} r_e\right) \right] \right\} = 0. \tag{45}$$

From Equation (45), it follows the following equation:

$$C_1 = -\frac{r_e{}^2}{r_e{}^2 - r_w{}^2}. \tag{46}$$

Owing to

$$\begin{cases} \int J_1(a \cdot r) dr = -\dfrac{J_0(a \cdot r)}{a}, \\ \int Y_1(a \cdot r) dr = -\dfrac{Y_0(a \cdot r)}{a}, \end{cases} \tag{47}$$

Table 3: Estimation of GIP by DMBM-APGR with $G_0 = 1.63828893 \times 10^8$ m^3 for the constant flow rate case.

No.	G_0 (m^3)	b [×10 MPa/(10^4 m^3/d)]	$-m_{mbe}$ [×10^{-3} MPa/(10^4 m^3)]	G_e (m^3)	E_a (%)
1	163828893	1.084881082	2.829760412	156613029	3.098
2	156613029	1.084665217	2.831432851	156520522	3.038
3	156520522	1.084662307	2.831455518	156519269	3.037
4	156519269	1.084662268	2.831455733	156519258	3.037
5	156519258	1.084662268	2.831455733	156519258	3.037

Table 4: Estimation of gas in place by DMBM-APGR with $G_0 = 0.3 \times 10^8$ m^3 for the constant flow rate case.

No.	G_0 (m^3)	b [×10 MPa/(10^4 m^3/d)]	$-m_{mbe}$ [×10^{-3} MPa/(10^4 m^3)]	G_e (m^3)	E_a (%)
1	30000000	1.089601043	2.793207447	158662526	4.448
2	158662526	1.084728730	2.830940857	156547724	3.055
3	156547724	1.084663163	2.831448987	156519631	3.037
4	156519631	1.084662279	2.831455666	156519261	3.037
5	156519261	1.084662268	2.831455733	156519258	3.037

Table 5: Estimation of gas in place by DMBM-APGR with $G_0 = 7.5 \times 10^8$ m^3 for the constant flow rate case.

No.	G_0 (m^3)	b [×10 MPa/(10^4 m^3/d)]	$-m_{mbe}$ [×10^{-3} MPa/(10^4 m^3)]	G_e (m^3)	E_a (%)
1	750000000	1.088235883	2.803775835	158064473	4.054
2	158064473	1.084710384	2.831082929	156539868	3.050
3	156539868	1.084662916	2.831450681	156519537	3.037
4	156519537	1.084662276	2.831455678	156519261	3.037
5	156519261	1.084662268	2.831455733	156519258	3.037

by integrating Equation (44) with respect to r, one obtains the following:

$$p_p = -\frac{q_m \mu_i B_{gi}}{\alpha_p K h}\left(\frac{1}{r_e^2 - r_w^2}\frac{r^2}{2} + C_1 \ln r + C_2\right) - \frac{\mu_i B_{gi}}{\alpha_p K h} \times \sum_{i=1}^{m}(q_i - q_{i-1}) \cdot \left\{\sum_{n=1}^{\infty}\frac{\pi}{\lambda_n} f(t_a, \lambda_n)\left[-Y_1(\lambda_n)J_0\left(\frac{\lambda_n}{r_w}r\right) + J_1(\lambda_n)Y_0\left(\frac{\lambda_n}{r_w}r\right)\right]\right\}. \tag{48}$$

Setting $r = r_w$, the equation above can be transformed into the following:

$$p_{p_{wf}} = -\frac{q_m \mu_i B_{gi}}{\alpha_p K h}\left(\frac{1}{r_e^2 - r_w^2}\frac{r_w^2}{2} + C_1 \ln r_w + C_2\right) - \frac{\mu_i B_{gi}}{\alpha_p K h} \times \sum_{i=1}^{m}(q_i - q_{i-1}) \cdot \left\{\sum_{n=1}^{\infty}\frac{\pi}{\lambda_n} f(t_a, \lambda_n)[-Y_1(\lambda_n)J_0(\lambda_n) + J_1(\lambda_n)Y_0(\lambda_n)]\right\}. \tag{49}$$

Subtracting Equation (49) from Equation (48) and combining it with Equations (31) and (46), we obtain the following:

$$p_p - p_{p_{wf}} = \frac{q_m \mu_i B_{gi}}{\alpha_p K h (r_e^2 - r_w^2)}\left(r_e^2 \ln\frac{r}{r_w} - \frac{r^2 - r_w^2}{2}\right) - \frac{\mu_i B_{gi}}{\alpha_p K h} \times \sum_{i=1}^{m}(q_i - q_{i-1}) \cdot \left\{\sum_{n=1}^{\infty} f(t_a, \lambda_n)\left[-\frac{\pi}{\lambda_n}Y_1(\lambda_n)J_0\left(\frac{\lambda_n}{r_w}r\right) + \frac{\pi}{\lambda_n}J_1(\lambda_n)Y_0\left(\frac{\lambda_n}{r_w}r\right) - \frac{2}{\lambda_n^2}\right]\right\}. \tag{50}$$

Table 6: Production schedules for the constant pressure case.

t (d)	TS	Δt (h)	Δt (d)	p_{wf} (MPa)
	1~12	1	0.041667	30
	13	3	0.125	30
1~1097	14	9	0.375	30
	15~16	12	0.5	30
	17~1111	24	1	30

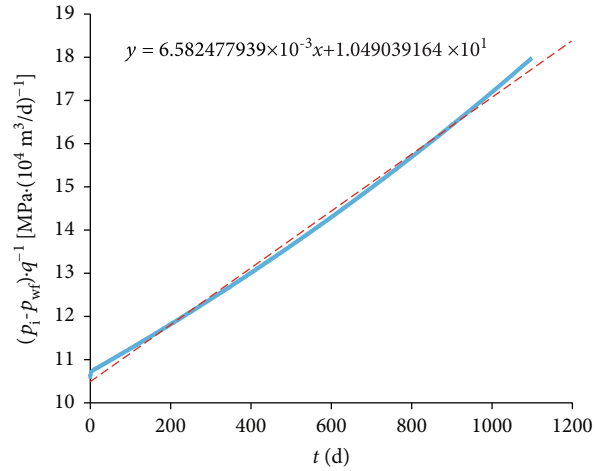

Figure 6: $(p_i - p_{wf}) \cdot q^{-1}$ vs. t for the constant pressure case.

Table 7: Estimation of GIP by DMBM-APGR with $G_0 = 126756360\ \mathrm{m}^3$ for the constant pressure case.

No.	G_0 (m^3)	$b\ [\times 10\ \mathrm{MPa}/(10^4\ \mathrm{m}^3/\mathrm{d})]$	$-m_{\mathrm{mbe}}\ [\times 10^{-3}\ \mathrm{MPa}/(10^4\ \mathrm{m}^3)]$	G_e (m^3)	E_a (%)
1	126756360	1.077118988	2.876528741	154066720	1.422
2	154066720	1.078496486	2.866998782	154578841	1.759
3	154578841	1.078517120	2.866855990	154586540	1.764
4	154586540	1.078517429	2.866853936	154586651	1.764
5	154586651	1.078517434	2.866853910	154586653	1.764
6	154586653	1.078517434	2.866853910	154586653	1.764

Table 8: Estimation of GIP by DMBM-APGR with $G_0 = 0.3 \times 10^8\ \mathrm{m}^3$ for the constant pressure case.

No.	G_0 (m^3)	$b\ [\times 10\ \mathrm{MPa}/(10^4\ \mathrm{m}^3/\mathrm{d})]$	$-m_{\mathrm{mbe}}\ [\times 10^{-3}\ \mathrm{MPa}/(10^4\ \mathrm{m}^3)]$	G_e (m^3)	E_a (%)
1	30000000	1.087541720	2.804493892	158024002	4.027
2	158024002	1.078652040	2.865922814	154636875	1.798
3	154636875	1.078519449	2.866839876	154587409	1.765
4	154587409	1.078517464	2.866853702	154586664	1.764
5	154586664	1.078517434	2.866853910	154586653	1.764

Table 9: Estimation of GIP by DMBM-APGR with $G_0 = 7.5 \times 10^8\ \mathrm{m}^3$ for the constant pressure case.

No.	G_0 (m^3)	$b\ [\times 10\ \mathrm{MPa}/(10^4\ \mathrm{m}^3/\mathrm{d})]$	$-m_{\mathrm{mbe}}\ [\times 10^{-3}\ \mathrm{MPa}/(10^4\ \mathrm{m}^3)]$	G_e (m^3)	E_a (%)
1	750000000	1.082955579	2.836168731	156259162	2.865
2	156259162	1.078583758	2.866395097	154611397	1.781
3	154611397	1.078518427	2.866847062	154587022	1.765
4	154587022	1.078517449	2.866853779	154586660	1.764
5	154586660	1.078517434	2.866853910	154586653	1.764

Based on Equation (50), the quasipressure p_p can be rewritten as follows:

$$p_p = A(r) + B(r), \tag{51}$$

$$A(r) = p_{p_{\mathrm{wf}}} + \frac{q_m \mu_i B_{\mathrm{gi}}}{\alpha_p K h (r_e^2 - r_w^2)} \left(r_e^2 \ln \frac{r}{r_w} - \frac{r^2 - r_w^2}{2} \right), \tag{52}$$

$$B(r) = -\frac{\mu_i B_{\mathrm{gi}}}{\alpha_p K h} \cdot \sum_{i=1}^{m} (q_i - q_{i-1}) \cdot \left\{ \sum_{n=1}^{\infty} f(t_a, \lambda_n) \left[-\frac{\pi}{\lambda_n} Y_1(\lambda_n) J_0\left(\frac{\lambda_n}{r_w} r\right) + \frac{\pi}{\lambda_n} J_1(\lambda_n) Y_0\left(\frac{\lambda_n}{r_w} r\right) - \frac{2}{\lambda_n^2} \right] \right\}. \tag{53}$$

The definition of average reservoir quasipressure is given by the following:

$$\left(p_p\right)_{\mathrm{ave}} = \frac{1}{\pi (r_e^2 - r_w^2)} \int_{r_w}^{r_e} p_p \cdot 2\pi r \cdot dr. \tag{54}$$

Table 10: Complex production schedules.

t (d)	TS	Δt (h)	Δt (d)	Production scenarios
	1~12	1	0.041667	
	13	3	0.125	
1~251	14	9	0.375	$q = 2.0 \times 10^4\ \mathrm{m}^3/\mathrm{d}$
	15~16	12	0.5	
	17~265	24	1	
252~592	266~606	24	1	$p_{\mathrm{wf}} = 30.9$ MPa
593~842	607~856	24	1	$q = 1.7 \times 10^4\ \mathrm{m}^3/\mathrm{d}$
843~1097	857-1111	24	1	$p_{\mathrm{wf}} = 2\,8.8$ MPa

By substituting Equation (51) into Equation (54), one obtains the following:

$$\begin{aligned} \left(p_p\right)_{\mathrm{ave}} &= I_1 + I_2 \\ &= \frac{2}{r_e^2 - r_w^2} \int_{r_w}^{r_e} A(r) \cdot r \cdot dr + \frac{2}{r_e^2 - r_w^2} \int_{r_w}^{r_e} B(r) \cdot r \cdot dr, \end{aligned} \tag{55}$$

where I_1 and I_2 are the integral formulas related to $A(r)$ and $B(r)$, respectively.

According to Equation (52), I_1 can be expressed as follows:

$$I_1 = \frac{2}{r_e^2 - r_w^2}\int_{r_w}^{r_e}\left[p_{p_{wf}} + \frac{q_m\mu_i B_{gi}}{\alpha_p Kh(r_e^2 - r_w)^2}\left(r_e^2 \ln\frac{r}{r_w} - \frac{r^2 - r_w^2}{2}\right)\right]\cdot r\cdot dr$$
$$= p_{p_{wf}} + \frac{2}{r_e^2 - r_w^2}\cdot\frac{q_m\mu_i B_{gi}}{\alpha_p Kh(r_e^2 - r_w^2)}\int_{r_w}^{r_e}\left(r_e^2 \ln\frac{r}{r_w} - \frac{r^2 - r_w^2}{2}\right)\cdot r\cdot dr. \tag{56}$$

Due to

$$\int_{r_w}^{r_e}\left(r_e^2 \ln\frac{r}{r_w} - \frac{r^2 - r_w^2}{2}\right)\cdot r\cdot dr = \frac{r_e^2 r_w^2}{2} + \frac{r_e^4}{2}\ln\frac{r_e}{r_w} - \frac{3}{8}r_e^4 - \frac{r_w^4}{8}, \tag{57}$$

Equation (56) can be transformed into the following:

$$I_1 = p_{p_{wf}} + \frac{q_m\mu_i B_{gi}}{\alpha_p Kh}\cdot\frac{4r_e^4\ln(r_e/r_w) - 3r_e^4 + 4r_e^2 r_w^2 - r_w^4}{4(r_e^2 - r_w^2)^2}. \tag{58}$$

According to Equation (53), analogously, I_2 can be expressed as follows:

$$I_2 = \frac{2}{r_e^2 - r_w^2}\int_{r_w}^{r_e}B(r)\cdot r\cdot dr$$
$$= -\frac{\mu_i B_{gi}}{\alpha_p Kh}\frac{2}{r_e^2 - r_w^2}\sum_{i=1}^{m}(q_i - q_{i-1})$$
$$\cdot\left\{\sum_{n=1}^{\infty}f(t_a,\lambda_n)\int_{r_w}^{r_e}\left[-\frac{\pi}{\lambda_n}Y_1(\lambda_n)J_0\left(\frac{\lambda_n}{r_w}r\right) + \frac{\pi}{\lambda_n}J_1(\lambda_n)Y_0\left(\frac{\lambda_n}{r_w}r\right) - \frac{2}{\lambda_n^2}\right]\cdot r\cdot dr\right\}. \tag{59}$$

Then, the equation above can be transformed into the following:

$$I_2 = -\frac{\mu_i B_{gi}}{\alpha_p Kh}\frac{2}{r_e^2 - r_w^2}\sum_{i=1}^{m}(q_i - q_{i-1})\left[\sum_{n=1}^{\infty}f(t_a,\lambda_n)\cdot\left(-\frac{r_e^2 - r_w^2}{\lambda_n^2}\right)\right]$$
$$= \frac{\mu_i B_{gi}}{\alpha_p Kh}\sum_{i=1}^{m}(q_i - q_{i-1})\left[\sum_{n=1}^{\infty}f(t_a,\lambda_n)\cdot\frac{2}{\lambda_n^2}\right]. \tag{60}$$

Substituting Equations (58) and (60) into Equation (55) yields the following:

$$(p_p)_{ave} = p_{p_{wf}} + \frac{q_m\mu_i B_{gi}}{\alpha_p Kh}\cdot\frac{4r_e^4\ln(r_e/r_w) - 3r_e^4 + 4r_e^2 r_w^2 - r_w^4}{4(r_e^2 - r_w^2)^2}$$
$$+ \frac{\mu_i B_{gi}}{\alpha_p Kh}\sum_{i=1}^{m}(q_i - q_{i-1})\left[\sum_{n=1}^{\infty}f(t_a,\lambda_n)\cdot\frac{2}{\lambda_n^2}\right]. \tag{61}$$

Assume $(p_p)_{ave} \approx p_{p_{ave}} = p_p(p_{ave})$, then divide both ends of Equation (61) by q_m, and eventually acquire the following expression:

$$\frac{p_{p_{ave}} - p_{p_{wf}}}{q_m} = \frac{\mu_i B_{gi}}{\alpha_p Kh}\cdot\frac{4r_e^4\ln(r_e/r_w) - 3r_e^4 + 4r_e^2 r_w^2 - r_w^4}{4(r_e^2 - r_w^2)^2}$$
$$+ \frac{\mu_i B_{gi}}{\alpha_p Kh}\sum_{i=1}^{m}\frac{q_i - q_{i-1}}{q_m}\left[\sum_{n=1}^{\infty}f(t_a,\lambda_n)\cdot\frac{2}{\lambda_n^2}\right], \tag{62}$$

where $p_{p_{ave}}$ or $p_p(p_{ave})$ denotes the quasipressure corresponding to average reservoir pressure.

According to Equation (36), Equation (62) can be rewritten as follows:

$$\frac{p_{p_{ave}} - p_{p_{wf}}}{q_m} = b, \tag{63}$$

or

$$p_{p_{ave}} = p_{p_{wf}} + q\cdot b. \tag{64}$$

The above derivation process has cogently proved the dynamic material balance equation for abnormally pressured gas reservoirs, i.e., Equation (64), which indicates that one can infer what the average reservoir quasipressure should be from the downhole quasipressure, indirectly capturing the intrinsic connection between the average formation pressure and the flowing bottomhole pressure. The dynamic material balance equation here is almost consistent with Matter's variable rate flowing material balance equation derived from gas flow equation for boundary-dominated flow, namely, stabilized flow, and MBE of volumetric gas reservoirs; however, our derivation procedure embodies the pore shrinkage of reservoir rock and the volume expansion of irreducible water based on a new definition of total compressibility and variable rate gas flow theory.

According to Equation (39), it is necessary to comprehend the average reservoir pressure data over time in order

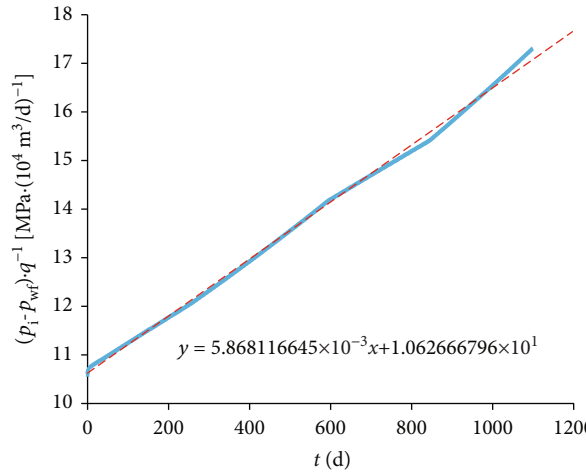

FIGURE 7: $(p_i - p_{wf})\cdot q^{-1}$ vs. t for the complex production schedules.

Table 11: Estimation of GIP by DMBM-APGR with $G_0 = 142187178\ \mathrm{m}^3$ for the complex production schedules.

No.	G_0 (m^3)	$b\left[\times 10\ \mathrm{MPa}/\left(10^4\ \mathrm{m}^3/\mathrm{d}\right)\right]$	$-m_{\mathrm{mbe}}\left[\times 10^{-3}\ \mathrm{MPa}/\left(10^4\ \mathrm{m}^3\right)\right]$	G_e (m^3)	E_a (%)
1	142187178	1.081131147	2.842097114	155933218	2.651
2	155933218	1.081700128	2.837955227	156160797	2.801
3	156160797	1.081708608	2.837893486	156164194	2.803
4	156164194	1.081708735	2.837892573	156164244	2.803
5	156164244	1.081708737	2.837892543	156164246	2.803
6	156164246	1.081708737	2.837892543	156164246	2.803

Table 12: Estimation of GIP by DMBM-APGR with $G_0 = 0.3 \times 10^8\ \mathrm{m}^3$ for the complex production schedules.

No.	G_0 (m^3)	$b\left[\times 10\ \mathrm{MPa}/\left(10^4\ \mathrm{m}^3/\mathrm{d}\right)\right]$	$-m_{\mathrm{mbe}}\left[\times 10^{-3}\ \mathrm{MPa}/\left(10^4\ \mathrm{m}^3\right)\right]$	G_e (m^3)	E_a (%)
1	30000000	1.089722537	2.779612157	159438556	4.958
2	159438556	1.081827761	2.837026254	156211931	2.834
3	156211931	1.081710510	2.837879593	156164959	2.803
4	156164959	1.081708763	2.837892376	156164255	2.803
5	156164255	1.081708737	2.837892543	156164246	2.803

Table 13: Estimation of GIP by DMBM-APGR with $G_0 = 7.5 \times 10^8\ \mathrm{m}^3$ for the complex production schedules.

No.	G_0 (m^3)	$b\left[\times 10\ \mathrm{MPa}/\left(10^4\ \mathrm{m}^3/\mathrm{d}\right)\right]$	$-m_{\mathrm{mbe}}\left[\times 10^{-3}\ \mathrm{MPa}/\left(10^4\ \mathrm{m}^3\right)\right]$	G_e (m^3)	E_a (%)
1	750000000	1.085874818	2.807581286	157850229	3.913
2	157850229	1.081770712	2.837441372	156189077	2.819
3	156189077	1.081709660	2.837885821	156164616	2.803
4	156164616	1.081708750	2.837892509	156164248	2.803
5	156164248	1.081708737	2.837892543	156164246	2.803

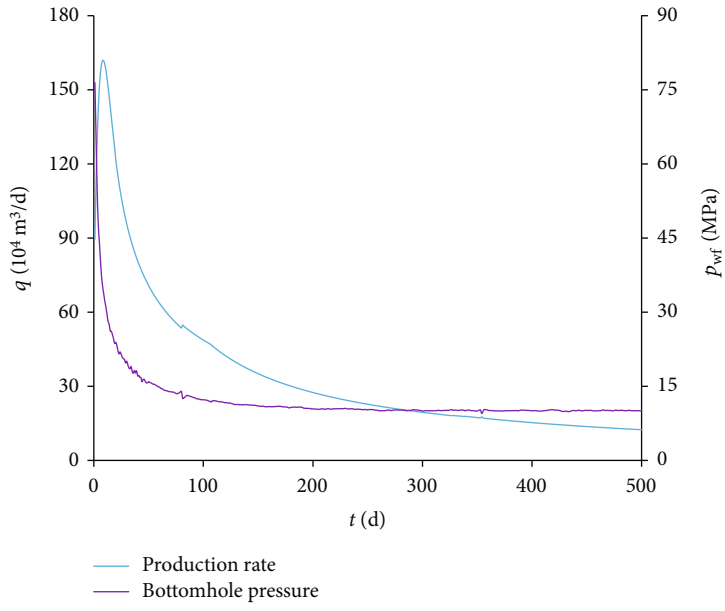

Figure 8: q and p_{wf} vs. t for gas well H-58.

to calculate t_{ca}, but p_{ave} values are often difficult to measure. Therefore, the iterative method, where an initial GIP value is postulated to calculate the p_{ave} and t_{ca} data and then GIP is updated by these data time and again, can be employed to determine the gas reserves. The average reservoir pressure p_{ave} could be determined by the (static) material balance equation of abnormally pressured gas reservoirs which will be introduced below.

3. Material Balance Equation for Abnormally Pressured Gas Reservoirs

For an overpressured gas reservoir, as a closed system, it is reasonable to assume that the invasion of edge or bottom water is negligible. Its material balance principle, therefore, can be phrased that natural gas production is mainly caused by the expansion of gas volume, bound water expansion, and the reduction in rock pore volume:

$$G_p B_g = \Delta V_w + \Delta V_p + G\left(B_g - B_{gi}\right), \tag{65}$$

where G_p (m^3) denotes the cumulative gas production, G (m^3) represents the gas in place or gas reserves, B_g (m^3/m^3) represents the gas formation volume factor, B_{gi} (m^3/m^3) is the gas formation volume factor under original reservoir condition, ΔV_p (m^3) is the reduced pore volume, and ΔV_w (m^3) denotes the expanded bound water volume.

From Equations (5) and (9), one obtains the following:

$$\Delta V_p = V_{pi} - V_p = V_{pi}\left[1 - e^{C_\phi(p_{ave}-p_i)}\right], \tag{66}$$

$$\Delta V_w = V_w - V_{wi} = V_{wi}\left[e^{-C_w(p_{ave}-p_i)} - 1\right]. \tag{67}$$

Pore volume and bound water volume under initial reservoir condition can be expressed, respectively, as follows:

$$\begin{aligned} V_{pi} &= \frac{GB_{gi}}{1 - S_{wci}}, \\ V_{wi} &= \frac{GB_{gi}}{1 - S_{wci}} S_{wci}. \end{aligned} \tag{68}$$

Gas formation volume factor is given by the following:

$$\begin{aligned} B_g(p_{ave}) &= \frac{ZT}{p_{ave}} \cdot \frac{p_{sc}}{Z_{sc}T_{sc}}, \\ B_{gi} &= \frac{Z_i T_i}{p_i} \cdot \frac{p_{sc}}{Z_{sc}T_{sc}}, \end{aligned} \tag{69}$$

where p_{sc} (1.01325×10^5 Pa), T_{sc} (293.15 K), and Z_{sc} denote the pressure, temperature, and deviation factor (Z-factor) under the standard condition, respectively; T_i is the initial reservoir temperature.

It is deemed justifiable that the temperature of the gas reservoir during its depletion nearly remains unchanged.

Table 14: Reservoir and gas properties for the field case.

Parameters	Property values
T_{pc}	200 K
p_{pc}	4.6 MPa
S_{wci}	0.2618
ϕ	0.1354
p_i	96.526602 MPa
T_i	3.664833×10^2 K
M_g	19.268256 g/mol
C_ϕ	8.702264×10^{-4} MPa^{-1}
C_w	5.801510×10^{-4} MPa^{-1}
μ_i	$4.751752304 \times 10^{-2}$ cp
Z_{sc}	0.997569589
Z_i	1.747395656
B_{gi}	$2.298698301 \times 10^{-3}$ m^3/m^3
C_{ti}	$3.589784792 \times 10^{-3}$ MPa^{-1}

Substituting Equations (66)–(69) into Equation (65) yields the following:

$$g(p_{ave}) = \frac{p_i}{Z_i}\left(1 - \frac{G_p}{G}\right), \tag{70}$$

$$g(p_{ave}) = \frac{p_{ave}}{Z(p_{ave})} \cdot \frac{e^{C_\phi(p_{ave}-p_i)} - S_{wci}e^{-C_w(p_{ave}-p_i)}}{1 - S_{wci}}, \tag{71}$$

where $g(p_{ave})$ denotes a function related to average reservoir pressure, defined by Equation (71).

The material balance equation for abnormally pressured gas reservoirs, i.e., Equation (70), expresses a relationship between the p_{ave}-dependent pressure function $g(p_{ave})$ in the overpressured gas reservoir and the cumulative gas production G_p, from which it can be observed that a straight-line section should appear on the $g(p_{ave})$ vs. G_p relationship curve with its intercept p_i/Z_i and the slope m_{mbe} or $-p_i/(Z_iG)$, helpful to determine the value of G. If the elastic effect of rock and bound water is insignificant, that is $C_w = C_\phi \approx 0$, then $g(p_{ave})$ can convert into $p_{ave}/Z(p_{ave})$, which is applicable to volumetric gas reservoirs. For overpressured gas reservoirs, nevertheless, the function $g(p_{ave})$ is supposed to be used; that is to say, it seems unreasonable to rashly apply $p_{ave}/Z(p_{ave}) \sim G_p$ relation to G estimation.

4. Dynamic Material Balance Method for Abnormally Pressured Gas Reservoirs

The relationships between Equations (34), (64), and (70) prompt us to calculate gas in place G, average reservoir pressure p_{ave}, and material balance quasitime t_{ca} by the iterative method shown in Figure 2. Its detailed steps are as follows:

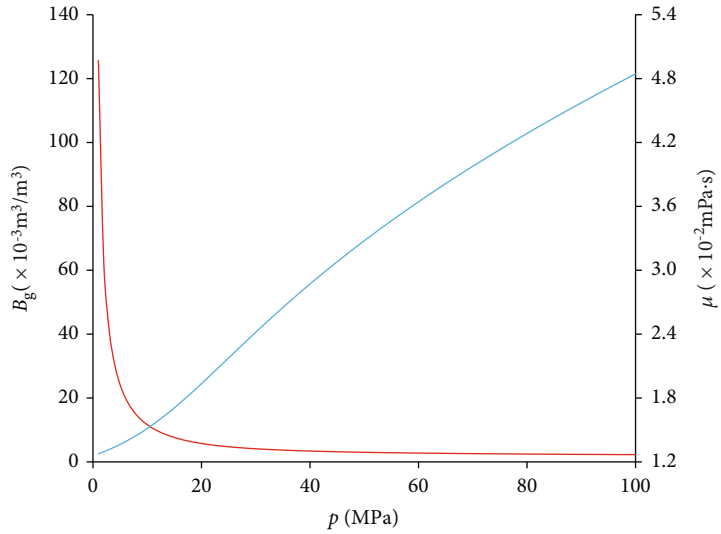

Figure 9: B_g and μ vs. p for the field case.

(1) Collect and sort out the known data available, such as gas production rate q, cumulative gas production G_p, and bottomhole pressure p_{wf}

(2) Use the slope of $(p_i - p_{wf})/q$ vs. t curve as m_{bdf} and estimate the initial GIP iteration value G_0 via Equation (38) (see Section 5.1.1 in the paper for details)

(3) Calculate the function $g(p_{ave})$ by Equation (70) and then determine p_{ave} according to Equation (71)

(4) Calculate t_{ca} by Equation (39), and total compressibility should be computed by Equation (12)

(5) Determine the intercept b of $(\Delta p_p)_{i-wf}/q$ vs. t_{ca} curve according to Equation (34)

(6) Estimate $p_p(p_{ave})$ by Equation (64) and then convert $p_p(p_{ave})$ into p_{ave} according to Equation (13)

(7) Calculate $g(p_{ave})$ by Equation (71), draw $g(p_{ave})$ vs. G_p relationship curve, and set the intercept of the straight line as p_i/Z_i, then use the slope m_{mbe} to determine the gas in place G_e

(8) Compare G_e calculated in Step 7 with the initial value G_0 in Step 2. If their difference meets accuracy requirement, then the estimated gas in place is G_e; otherwise, assign G_e to G_0 and repeat Steps 2 to 8

Owing to the application of dynamic material balance equation, i.e., Equation (64) and (static) material balance equation, i.e., Equation (70) to overpressured gas reservoirs, the above method for estimating gas in place is called DMBM-APGR (dynamic material balance method for abnormally pressured gas reservoirs) in the paper. It is inessential to shut the gas well or conduct a well testing destined for static pressure since the method only needs production data (q, p_{wf}, G_p, etc.) available to determine gas in place G, which boasts low cost and considerable convenience in that the computing process can be easily completed by programs and data sheets.

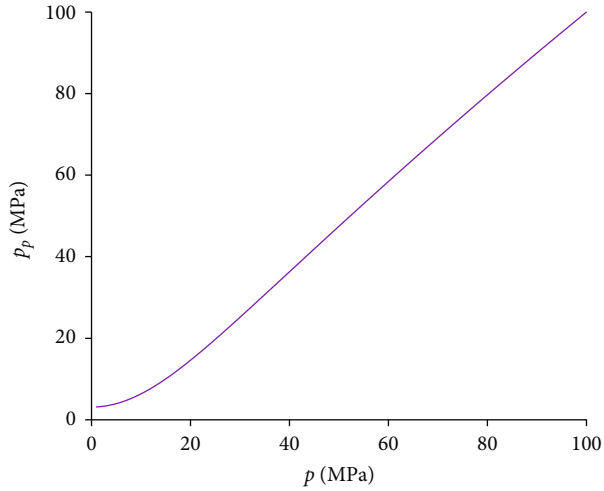

Figure 10: p_p vs. p for the field case.

5. Results and Discussion

5.1. Numerical Simulation Verification. Several numerical examples are listed below to illustrate the applicability of DMBM-APGR to overpressured gas reservoirs. We employ the black oil model to simulate the radial single-phase gas flow with a production well located in the center of a circular closed formation, considering the shrinkage of rock pore volume and the expansion of irreducible water volume. The radial grid type is $200 \times 72 \times 1$; the original reservoir pressure p_i is 55 MPa, the temperature T_i is 108°C, the initial rock porosity ϕ_i is 0.2, and the initial irreducible water saturation S_{wci} is 0.2. The depths of the top face of each grid block are set to 2995 m. The pore volume at initial reservoir condition V_{pi} and actual gas in place G obtained by initialization are 565864 m^3 and 1.51906310×10^8 m^3, respectively. Other

parameters about gas reservoir and natural gas are shown in Table 1.

In Table 1, dr denotes the radial length of the grid, $d\theta$ denotes the angular size of each grid block, and dz denotes the grid height; K_r, K_θ, and K_z are the radial permeability, azimuthal permeability, and vertical permeability, respectively; T_{pc} represents the pseudocritical temperature of gas mixture and p_{pc} represents the gas pseudocritical pressure.

The viscosity correlations proposed by Londono et al. (2002, 2005) [37, 38] are used to calculate the gas viscosity, and the Hall-Yarborough (1973) method [39] is used to determine the Z-factor and gas compressibility C_g. The resulting relation between gas formation volume factor B_g and pressure p and that between gas viscosity μ and p are shown in Figure 3. In line with Equation (13), Figure 4 reveals the relationship between quasipressure function p_p and pressure p.

5.1.1. Constant Production Rate Simulation. We set 1111-time steps, and the simulation period lasts about 3 years where the time intervals represented by time steps 1~12 are one hour, time steps 13 and 14 are 3 h and 9 h, respectively, and the time intervals of time steps 15 and 16 are 0.5 d. Other time steps' time intervals are all one day. The production rate of the gas well, a constant, was set to 1.6×10^4 m^3/d. The production schedules are shown in Table 2 where TS denotes time step and Δt represents time interval.

The time-dependent data such as production rate q, bottomhole flowing pressure p_{wf}, and cumulative gas production G_p, obtained by numerical simulation, can be readily recorded. Since the relationships between gas viscosity, deviation factor, and pressure are known, the quasipressure data corresponding to bottomhole pressure can be calculated according to Equation (13). Therefore, the ordinate plotting function $(\Delta p_p)_{i-wf}/q$ in Equation (34) can be also determined. Now, we only need to iteratively calculate the values of the abscissa plotting function t_{ca}.

To determine the material-balance quasitime t_{ca} requires a given GIP value G_0. This initial value of iteration can be determined by the slope of $(p_i - p_{wf})/q$ vs. t curve, that is, this slope can be used to replace m_{bdf} in Equation (38). As shown in Figure 5, when the quasipressure and quasitime are not used, the slope of $(p_i - p_{wf})/q$ vs. t curve is $5.092941367 \times 10^{-3}$ MPa $\cdot (10^4\ \text{m}^3)^{-1}$, so the GIP estimated by the slope is 163828893 m^3 according to Equation (39), which can be used as the initial iteration value. The relevant results by DMBM-APGR are shown in Table 3.

In Table 3, G_e is the GIP determined by G_0 during the same iteration step, and E_a is the estimation error of GIP defined by the following equation:

$$E_a = \frac{G_e - G}{G} \times 100\%. \tag{72}$$

If the real pressure and real time are used directly, as mentioned above, the GIP value calculated by the slope of the straight line in $(p_i - p_{wf})/q$ vs. t graph is 163828893 m^3 which is 7.849% larger than the real GIP. The GIP values estimated by DMBM-APGR, however, gradually stabilize to 156519258 m^3, and the error is merely 3.037% satisfactory for reservoir engineering. The difference between two adjacent estimated values after two iterations, in fact, is small enough to terminate calculation. Though the initial iteration values of GIP are far away from the real value G, the estimation by DMBM-APGR will tend to be the same result (see Tables 4 and 5).

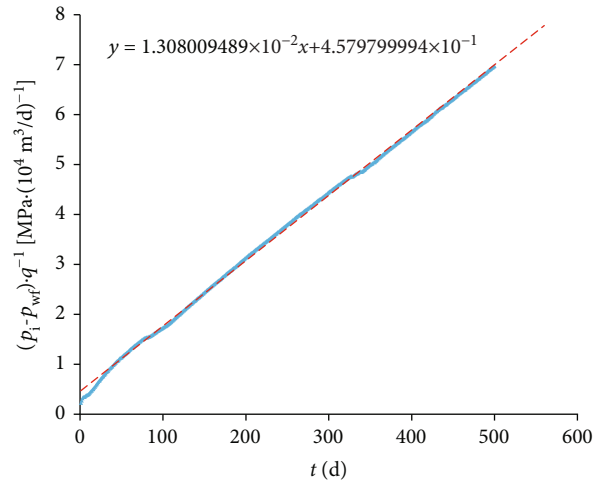

FIGURE 11: $(p_i - p_{wf})/q$ vs. t relationship for the field case.

5.1.2. Constant Bottomhole Pressure Simulation. Setting the production schedule of gas well as "$p_{wf} = 30$ MPa" without changes in other parameters generates the constant pressure production case as shown in Table 6. According to the simulation results, the slope of $(p_i - p_{wf})/q$ vs. t curve is $6.582477939 \times 10^{-3}$ MPa$\cdot(10^4\ \text{m}^3)^{-1}$ as shown in Figure 6, so the GIP estimation from this slope is 126756360 m^3 with an unacceptable error of -16.556%. The estimation, nonetheless, can serve as the initial value of iteration, and the resulting calculation results by DMBM-APGR are shown in Table 7.

Table 7 indicates that it only takes two iterations for DMBM-APGR to achieve the expected accuracy in that the difference between the GIP estimation in 2nd iteration and that in 1st iteration is merely 0.332%, and then the calculation could be terminated. If the iterative process continues, the ultimate results will become 154586653 m^3 with an error of 1.764%. The calculation results, when selecting other values as the initial value of iteration, are shown in Tables 8 and 9.

It can be seen from Tables 8 and 9 that no matter how the initial iteration value is set, the final GIP estimation will stabilize to 154586653 m^3. In general, the calculation process can just cease after three iterations because the difference between two adjacent iterations is small enough. The calculated results in Tables 7–9 prove that DMBM-APGR is also applicable to the production systems at constant bottomhole pressure.

5.1.3. Complex Production Schedules. It is not hard to discover from the previous two calculation examples that

Table 15: Estimation of GIP by DMBM-APGR with $G_0 = 1.572152725 \times 10^8\ \mathrm{m}^3$ for the field case.

No.	$G_0\ (\times 10^8\ \mathrm{m}^3)$	$b\ [\times 10^{-1}\ \mathrm{MPa}/(10^4\ \mathrm{m}^3/\mathrm{d})]$	$-m_{\mathrm{mbe}}\ [\times 10^{-3}\ \mathrm{MPa}/(10^4\ \mathrm{m}^3)]$	$G_e\ (\times 10^8\ \mathrm{m}^3)$	E_d (%)
1	1.572152725	13.33851026	1.519438872	3.635570192	131.248
2	3.635570192	9.147892147	1.889344623	2.923779286	-19.579
3	2.923779286	8.318160846	1.973922926	2.798501704	-4.285
4	2.798501704	8.131995777	1.993513905	2.770999820	-0.983
5	2.770999820	8.089188246	1.998050758	2.764707878	-0.227

Table 16: Estimation of GIP by DMBM-APGR with $G_0 = 0.15 \times 10^8\ \mathrm{m}^3$ for the field case.

No.	$G_0\ (\times 10^8\ \mathrm{m}^3)$	$b\ [\times 10^{-1}\ \mathrm{MPa}/(10^4\ \mathrm{m}^3/\mathrm{d})]$	$-m_{\mathrm{mbe}}\ [\times 10^{-3}\ \mathrm{MPa}/(10^4\ \mathrm{m}^3)]$	$G_e\ (\times 10^8\ \mathrm{m}^3)$	E_d (%)
1	0.15	11.71822396	1.651891156	3.344062139	2129
2	3.344062139	8.849559927	1.919260635	2.878205582	-13.931
3	2.878205582	8.252071177	1.980846495	2.788720219	-3.109
4	2.788720219	8.116853242	1.995112895	2.768778993	-0.715
5	2.768778993	8.085699822	1.998420096	2.764196919	-0.165

DMBM-APGR manifests a desirable application effect for both constant rate and constant pressure production systems. For further verification, the gas well production under complex schedules is also simulated by setting several combinations of constant rate production and constant pressure production as shown in Table 10 on condition that the reservoir and gas properties remain unchanged. Like the former example, the estimated value of GIP by the slope of $(p_i - p_{wf})/q$ vs. t relationship (see Figure 7) is $142187178\ \mathrm{m}^3$, which can be used as the initial value of iteration. The corresponding calculated results by DMBM-APGR are shown in Table 11.

It can be seen from Table 11 that the change rate in estimated GIP after two iterations is clearly less than 1% with an acceptable calculation error of 2.801%, when setting initial iteration value $G_0 = 142187178\ \mathrm{m}^3$. If the iteration process continues, the estimated values will eventually stay at $156164246\ \mathrm{m}^3$. Tables 12 and 13 exhibit the calculation results when other initial values of iteration are given.

Similarly, the modifications to initial iteration values do not heavily affect the calculation accuracy of DMBM-APGR as can be seen from Tables 12 and 13, while the number of iterations to reach the termination condition may increase. The calculation process, in practice, can be terminated after 3 iterations, because the difference between two adjacent GIP estimations at that moment is less than 1%, and the calculation error is 2.803%. The calculation results for the complex production schedules, as shown in Tables 11–13, provide convincing evidence for the feasibility and validity of DMBM-APGR in those situations where production rate and bottomhole flowing pressure fluctuate slightly.

5.2. Field Case Verification. Figure 8 shows the production history for gas well H-58 presented by Ibrahim et al. (2003) [40] and Wang and Ayala (2020) [17]. The reservoir and gas properties for the well are listed in Table 14. Similar to the previous numerical cases, the HY (1973) method [39] is employed to estimate the Z-factor and gas compressibility C_g, and viscosity correlations developed by Londono et al. (2002, 2005) [37, 38] are used for gas viscosity calculations. Figure 9 shows the relationship between B_g and p and that between μ and p. Figure 10 exhibits the relationship between p_p and p, depicted by Equation (13).

The estimated value of GIP by the slope of $(p_i - p_{wf})/q$ vs. t relationship shown in Figure 11 is $1.572152725 \times 10^8\ \mathrm{m}^3$, which can be used as the initial value of iteration. The corresponding calculated results by DMBM-APGR are shown in Table 15. The difference between two adjacent GIP estimations is denoted by E_d:

$$E_d = \frac{G_e - G_0}{G_0} \times 100\%. \tag{73}$$

It can be seen from Table 15 that for a given initial iteration value of $1.572152725 \times 10^8\ \mathrm{m}^3$, the variation in estimated GIP after four iterations is less than 1% with an estimate of $2.771 \times 10^8\ \mathrm{m}^3$. Tables 16 and 17 exhibit the calculation results when other initial values of iteration are considered.

As shown in Figure 12, the estimated values will eventually stay at $2.762819832 \times 10^8\ \mathrm{m}^3$ if the above iteration process continues. The changes in initial iteration values have little effect on the calculation accuracy of DMBM-APGR for the field case. The calculation process, in fact, can be terminated after 4 iterations because E_d is less than 1% at that time. The above calculation results for the field case match well with the predicted value of $2.775050966 \times 10^8\ \mathrm{m}^3$ (or 9.8 Bcf) presented by Ibrahim et al. (2003) and the estimate of $2.690100426 \times 10^8\ \mathrm{m}^3$ (or 9.5 Bcf) by Wang and Ayala (2020), which further demonstrates the feasibility and applicability of DMBM-APGR during boundary-dominated flow though production rate and bottomhole pressure may fluctuate slightly.

Table 17: Estimation of GIP by DMBM-APGR with $G_0 = 15 \times 10^8$ m^3 for the field case.

No.	G_0 ($\times 10^8$ m^3)	b [$\times 10^{-1}$ MPa/(10^4 m^3/d)]	$-m_{mbe}$ [$\times 10^{-3}$ MPa/(10^4 m^3)]	G_e ($\times 10^8$ m^3)	E_d (%)
1	15	11.30476343	1.687722063	3.273066575	-78.180
2	3.273066575	8.768858534	1.927449221	2.865977797	-12.438
3	2.865977797	8.234025935	1.982754667	2.786036399	-2.789
4	2.786036399	8.112682580	1.995559002	2.768160033	-0.642
5	2.768160033	8.084726724	1.998523722	2.764053592	-0.148

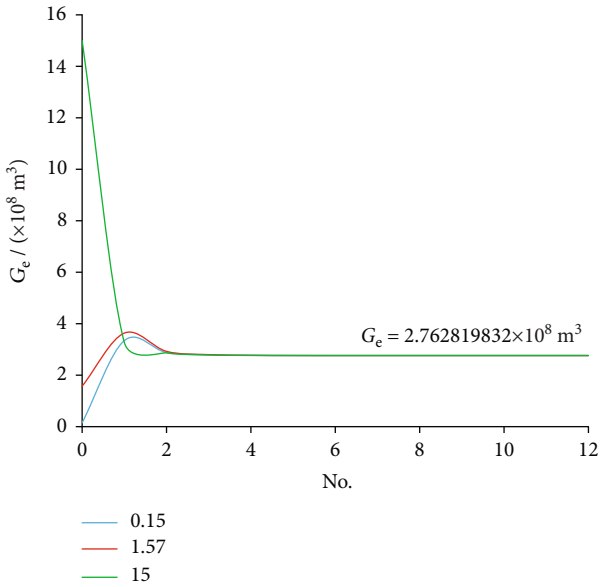

Figure 12: Iteration processes of DMBM-APGR with different initial values for the field case.

5.3. Discussion. There are many methods for determination of GIP, the majority of which, nevertheless, fail to calculate GIP of abnormally pressured gas reservoirs with low cost and acceptable accuracy. For example, the conventional material balance method needs average reservoir pressure data by shutting the gas well or conducting a well testing destined for static pressure. Most methods for production decline analysis (or rate transient analysis), however, do not consider the elastic effects of rock pore and irreducible water. As a matter of fact, both formation and water compressibility effects are supposed to be considered in the production performance analysis.

Therefore, this study is aimed at offering a reliable approach for determining gas reserves applicable to abnormally high-pressure gas reservoirs with desirable accuracy and low cost. The novelties of the work lie in the following. (1) The iterative method DMBM-APGR presented in the paper reckons with the influence of rock and water compressibility, and avoids well shutdown or well testing since it only requires production data (q, p_{wf}, G_p, etc.) available to determine G, which boasts low cost and high convenience. (2) The dynamic material balance equation is strictly derived from the gas flow model for a closed system with abnormally high pressure. (3) The method combines the static material balance equation with the dynamic material balance equation for overpressured gas reservoirs to design the iterative steps for GIP estimation. (4) A practical selection strategy of an initial iteration value of GIP is proposed though the method is not sensitive to choices of the initial value.

Three numerical cases and a field case validate the applicability of DMBM-APGR to overpressured gas reservoirs with constant production rate, constant bottomhole pressure, and variable rate/variable pressure conditions. The changes in initial iteration values have little effect on the calculation accuracy of DMBM-APGR for all the cases because the estimated GIP by the method always ultimately stabilizes to a fixed value independent of initial iteration values, which shows its robustness and reliability.

6. Conclusions

(1) A new definition of total compressibility, pertinent to the compressibilities of gas, rock, and irreducible water, is developed in this paper, and the dynamic material balance equation for abnormally pressured gas reservoirs is rigorously proved using the gas flow theory with a variable flow rate, too

(2) Based on the relationship between the quasipressure corresponding to bottomhole pressure and the one corresponding to average reservoir pressure (i.e., dynamic material balance equation) and the material balance principle of overpressured gas reservoirs, the authors present the dynamic material balance method for abnormally pressured gas reservoir (DMBM-APGR), an iterative method for calculating GIP of gas reservoirs without water drive by production data. The method not only considers the pore reduction in reservoir rock and the volume expansion of bound water, but also embodies the fluctuations in production rate and changes in gas properties

(3) Simulated cases under various production scenarios and a field case are used to verify the applicability and effectiveness of the method. The paper creatively proposes a selection strategy of an initial iteration value of GIP where initial value G_0 can be set as the estimated value calculated by the slope of $(p_i - p_{wf})/q$ vs. t straight line. Generally, the accuracy requirement can be fulfilled after 2 to 4 iterations using DMBM-APGR, and the calculation error of gas in place is less than 5%, acceptable and desirable for reservoir engineering application

(4) DMBM-APGR is not sensitive to the selection of the initial iteration value of GIP, and the estimated gas in place by the method will always ultimately stabilize to a fixed value, which shows that it is robust and reliable. It is recommended to adopt the selection strategy presented here for initial values of iteration; otherwise, the number of iterations to satisfy the stopping criterion may rise

Data Availability

The gas properties data used for numerical simulation and filed application are generated by Londono et al. [37, 38] and Hall-Yarborough [39] correlations (provided in Figures 3, 4, 9, and 10 in the manuscript). The simulated production data (such as production rate, bottomhole pressure, and cumulative gas production) under various scenarios are derived from *Eclipse*, a commercial reservoir simulator. The field case is derived from Wang and Ayala (2020) [17] and Ibrahim et al. (2003) [40].

Conflicts of Interest

The authors declare that they have no conflicts of interest.

Acknowledgments

This work has been supported by the Department of Asia-Pacific E&P and Department of Middle East E&P, Research Institute of Petroleum Exploration and Development, PetroChina. We gratefully acknowledge the financial support from the National Science and Technology Major Project of China (Grant No. 2017ZX05030-003). Our thanks also go to Jinyu Guo, Lang Li and Ping Chen for revision suggestions.

References

[1] A. Satter and G. M. Iqbal, *Reservoir Engineering: the Fundamentals, Simulation, and Management of Conventional and Unconventional Recoveries*, Gulf Professional Publishing, Waltham, 2016.

[2] F. E. Gonzalez and T. A. Blasingame, "A quadratic cumulative production model for the material balance of an abnormally pressured gas reservoir," in *SPE Western Regional and Pacific Section AAPG Joint Meeting*, pp. 1–33, Bakersfield, California, 2008.

[3] N. Q. Liu, *Practical Modern Well Test Interpretation*, Petroleum Industry Press, Beijing, 5th edition, 2008.

[4] Z. Wu, C. Cui, G. Lv, S. Bing, and G. Cao, "A multi-linear transient pressure model for multistage fractured horizontal well in tight oil reservoirs with considering threshold pressure gradient and stress sensitivity," *Journal of Petroleum Science and Engineering*, vol. 172, pp. 839–854, 2019.

[5] L. Mattar and D. M. Anderson, "A systematic and comprehensive methodology for advanced analysis of production data," in *SPE Annual Technical Conference and Exhibition*, pp. 1–14, Denver, Colorado, 2003.

[6] H. D. Sun, *Advanced Production Decline Analysis and Application*, Gulf Professional Publishing, Waltham, MA, 2015.

[7] Z. Wu, L. Dong, C. Cui, X. Cheng, and Z. Wang, "A numerical model for fractured horizontal well and production characteristics: comprehensive consideration of the fracturing fluid injection and flowback," *Journal of Petroleum Science and Engineering*, vol. 187, article 106765, 2020.

[8] L. Mattar and R. McNeil, "The "flowing" material balance procedure," in *46th Annual Technical Meeting of The Petroleum Society of CIM*, pp. 1–6, Banff in Alberta, 1995.

[9] L. Mattar and R. McNeil, "The "flowing" gas material balance," *Journal of Canadian Petroleum Technology*, vol. 37, no. 2, pp. 52–55, 1998.

[10] T. A. Blasingame and W. J. Lee, "Variable-rate reservoir limits testing of gas wells," in *SPE Gas Technology Symposium*, pp. 43–56, Dallas, Texas, 1988.

[11] L. Mattar and D. Anderson, "Dynamic material balance (oil or gas-in-place without shut-ins)," in *Petroleum Society's 6th Canadian International Petroleum Conference*, pp. 1–9, Calgary, 2005.

[12] L. Mattar and D. Anderson, "Dynamic material balance—oil- or gas-in-place without shut-ins," *Journal of Canadian Petroleum Technology*, vol. 45, no. 11, pp. 7–10, 2006.

[13] D. Ismadi, C. S. Kabir, and A. R. Hasan, "The use of combined static and dynamic material-balance methods in gas reservoirs," in *SPE Asia Pacific Oil and Gas Conference and Exhibition*, pp. 1–16, Jakarta, Indonesia, 2011.

[14] D. Ismadi, C. S. Kabir, and A. R. Hasan, "The use of combined static- and dynamic-material-balance methods with real-time surveillance data in volumetric gas reservoirs," *SPE Reservoir Evaluation & Engineering*, vol. 15, no. 3, pp. 351–360, 2012.

[15] M. Zhang and L. F. Ayala, "Gas-production-data analysis of variable-pressure-drawdown/variable-rate systems: a density-based approach," *SPE Reservoir Evaluation & Engineering*, vol. 17, no. 4, pp. 520–529, 2014.

[16] T. N. Stumpf and L. F. Ayala, "Rigorous and explicit determination of reserves and hyperbolic exponents in gas-well decline analysis," *SPE Journal*, vol. 21, no. 5, pp. 1843–1857, 2016.

[17] Y. Wang and L. F. Ayala, "Explicit determination of reserves for variable-bottomhole-pressure conditions in gas rate-transient analysis," *SPE Journal*, vol. 25, no. 1, pp. 369–390, 2019.

[18] T. L. Qin, D. Li, and Y. Q. Chen, *Practical Reservoir Engineering Methods*, Beijing: Petroleum Industry Press, 1989.

[19] Y. Q. Chen and D. Li, *Modern Petroleum Reservoir Engineering*, Beijing: Petroleum Industry Press, 2001.

[20] R. Al-Hussainy, H. J. Ramey, and P. B. Crawford, "The flow of real gases through porous media," *Journal of Petroleum Technology*, vol. 18, no. 5, pp. 624–636, 1966.

[21] R. Al-Hussainy and H. J. Ramey, "Application of real gas flow theory to well testing and deliverability forecasting," *Journal of Petroleum Technology*, vol. 18, no. 5, pp. 637–642, 1966.

[22] D. G. Russell, J. H. Goodrich, G. E. Perry, and J. F. Bruskotter, "Methods for predicting gas well performance," *Journal of Petroleum Technology*, vol. 18, no. 1, pp. 99–108, 1966.

[23] R. G. Agarwal, "Real gas pseudo-time - a new function for pressure buildup analysis of MHF gas wells," in *SPE Annual Technical Conference and Exhibition*, pp. 1–12, Las Vegas, Nevada, 1979.

[24] W. J. Lee and S. A. Holditch, "Application of pseudotime to buildup test analysis of low-permeability gas wells with long-

duration wellbore storage distortion," *Journal of Petroleum Technology*, vol. 34, no. 12, pp. 2877–2887, 1982.

[25] M. L. Fraim and R. A. Wattenbarger, "Gas reservoir decline-curve analysis using type curves with real gas pseudopressure and normalized time," *SPE Formation Evaluation*, vol. 2, no. 4, pp. 671–682, 1987.

[26] D. F. Meunier, C. S. Kabir, and M. J. Wittmann, "Gas well test analysis: use of normalized pressure and time functions," in *SPE Annual Technical Conference and Exhibition*, pp. 1–16, Houston, Texas, 1984.

[27] D. F. Meunier, C. S. Kabir, and M. J. Wittmann, "Gas well test analysis: use of normalized pseudovariables," *SPE Formation Evaluation*, vol. 2, no. 4, pp. 629–636, 1987.

[28] P. Ye and H. L. F. Ayala, "A density-diffusivity approach for the unsteady state analysis of natural gas reservoirs," *Journal of Natural Gas Science and Engineering*, vol. 7, pp. 22–34, 2012.

[29] P. Vardcharragosad and L. F. Ayala, "Rate-time forecasting of gas reservoirs with significant transient flow: a density-based method," *Journal of Unconventional Oil and Gas Resources*, vol. 11, pp. 111–126, 2015.

[30] P. J. Mohr, D. B. Newell, and B. N. Taylor, "CODATA recommended values of the fundamental physical constants: 2014," *Journal of Physical and Chemical Reference Data*, vol. 45, no. 4, article 043102, 2016.

[31] P. J. Mohr, D. B. Newell, and B. N. Taylor, "CODATA recommended values of the fundamental physical constants: 2014," *Reviews of Modern Physics*, vol. 88, no. 3, article 035009, 2016.

[32] X. Y. Kong, *Advanced Fluid Mechanics in Porous Medium*, University of Science and Technology of China Press, Hefei, 2010.

[33] T. A. Blasingame and W. J. Lee, "Variable-rate reservoir limits testing," in *Permian Basin Oil and Gas Recovery Conference*, pp. 361–369, Midland, Texas, 1986.

[34] D. M. Anderson and L. Mattar, "An improved pseudo-time for gas reservoirs with significant transient flow," in *Canadian International Petroleum Conference*, pp. 1–11, Calgary, Alberta, 2005.

[35] D. M. Anderson and L. Mattar, "An improved pseudo-time for gas reservoirs with significant transient flow," *Journal of Canadian Petroleum Technology*, vol. 46, no. 7, pp. 49–54, 2007.

[36] P. Ye and H. L. F. Ayala, "Straightline analysis of flow rate vs. cumulative-production data for the explicit determination of gas reserves," *Journal of Canadian Petroleum Technology*, vol. 52, no. 4, pp. 296–305, 2013.

[37] F. E. Londono, R. A. Archer, and T. A. Blasingame, "Simplified correlations for hydrocarbon gas viscosity and gas density - validation and correlation of behavior using a large-scale database," in *SPE Gas Technology Symposium*, pp. 1–16, Calgary, 2002.

[38] F. E. Londono, R. A. Archer, and T. A. Blasingame, "Correlations for hydrocarbon gas viscosity and gas density - validation and correlation of behavior using a large-scale database," *SPE Reservoir Evaluation & Engineering*, vol. 8, no. 6, pp. 561–572, 2005.

[39] K. R. Hall and L. Yarborough, "A new equation of state for Z-factor calculations," *Oil and Gas Journal*, vol. 71, no. 7, pp. 82–85, 90, 92, 1973.

[40] M. Ibrahim, R. A. Wattenbarger, and W. Helmy, "Determination of OGIP for wells in pseudosteady-state-old techniques, new approaches," in *SPE Annual Technical Conference and Exhibition*, pp. 1–12, Denver, Colorado, 2003.